18

Molecular Sieve–Based Materials for Photonic Applications

Katrin Hoffmann
Federal Institute for Materials Research and Testing (BAM), Berlin, Germany

Frank Marlow
Max Planck Institute for Coal Research, Mülheim an der Ruhr, Germany

I. INTRODUCTION

Communication systems have been dominated by electronic processes, but photonic concepts are increasingly gaining importance in information technology with devices such as lasers, light-emitting diodes, photodetecting diodes, optical switches, optical amplifiers, optical modulators, and optical fibers. The aim of the efforts is to reduce the size of optical devices and to integrate them jointly on a single optical circuit.

Optical materials for photonic purposes are made to change the flow of light by interaction with the electronic states of the materials. Separation of the complex process into subfunctions supported by different components of an optical material allows efficient tuning of the interaction with the photons, resulting in optimized optical parameters.

Organic/inorganic hybrid materials such as composites from molecular sieve crystals and organic guests have been undergoing developments in the area of material research for advanced applications (1–7). The nano-sized channel system of molecular sieves provides a size- and shape-selective matrix for adsorbates organized and oriented in the nanometer scale. Because of the unique properties due to the highly ordered arrangements of guest molecules, the resulting zeolitic composites are very interesting materials for novel electrical (8) and photonic (9) applications. The modular composition of zeolitic hybrid materials should enable a very efficient design of optical materials because of an independent tuning possibility on every length scale involved in complex optical functionalities.

In this chapter, design and optical characterization of individual composite crystals are reported with a special focus on composite crystals that must be large enough for photonic applications. The novel optical properties of these materials, such as optical second harmonic generation, laser properties, and reversible switching are being presented. Investigations on materials suitable for optical switching are here described in detail.

II. COMPOSITION OF ZEOLITIC ORGANIC/INORGANIC HYBRID MATERIALS

A. Synthesis of Large Zeolite Crystals for Photonic Applications

The synthesis of zeolites for classical applications such as ion exchange in detergents, adsorption, or catalysis requires small micrometer-sized crystals to reduce diffusion problems. Numerous ways of reducing the mean particle size are reported. They also meet economic demands, such as short crystallization time, and deliver narrow particle size distribution (10).

The requirements on zeolitic materials as hosts for functional guest molecules in novel electrical and optical nanodevices are usually quite different from the demands in classical applications, especially with regard to their macroscopic shape. Common zeolite powders are not suitable for most optical applications because of strong scattering effects. The light scattering losses can be reduced (a) by immersion in nonabsorbing media of similar refractive indices or (b) by decrease in the particle size. Therefore, the zeolite powders have been immersed in solvents (11) or in organic polymers (12,13). Suspensions can also be stabilized by modifying the surfaces of nanocrystalline zeolite particles (14). All methods result in transparent systems useful for optical and spectroscopic investigations. Especially crystals embedded in polymer films would be easy to handle in optical devices. These transparent films are an important step in the development of materials showing minimized scattering losses. In addition, there has been considerable research effort in the synthesis of large, optically perfect zeolite crystals for advanced, especially photonic, applications.

1. Defects

Intracrystalline defects directly influence the diffusion of guest molecules and the formation of an ordered intrazeolitic arrangement of adsorbates. Since the optical and electronic effects depend strongly on this arrangement, especially photonic applications are sensitive to intracrystalline disorder. Therefore, well-shaped zeolite single crystals with few defects are necessary. In addition, the crystals should be optically clear in the ultraviolet (UV) and visible (VIS) spectral region to avoid scattering losses at intracrystalline boundaries.

Apart from scattering losses which reduce the optical UV transparency, microporous siliceous materials show an onset of absorption of electromagnetic radiation in the UV spectral range around 280 nm, although dense SiO_2 phases are transparent down to 180 nm. This absorption was attributed to defects in the zeolite lattice. Structural defects, similar to those found in amorphous silica, should also exist in crystalline samples where the silicon atoms are coordinated tetrahedrally by oxygen. Especially peroxy radicals and/or peroxy bridges can form E′ centers, which are known to absorb light in the region of 160 to about 300 nm. The calcination of zeolitic materials, which is necessary to remove the organic template and make the pore system accessible for functional guest molecules, increases the short-wavelength absorption due to defect generation or minor amounts of organic residues withstanding the calcination process. Using template-free synthesis procedures, defect-free but, unfortunately, very small molecular sieve crystals that are completely transparent down to 200 nm have been obtained (15).

The hydrothermal synthesis of silicoaluminophosphate molecular sieve crystals with AFI structure is very sensitive to the synthesis conditions and the starting materials. Large crystals with a high optical quality result only if an aluminum oxide hydrate sol or pseudohydrargillite was used as aluminum source. The incorporation of silicon in the

AFI framework (SAPO-5) controls the optical transparency, the morphology, and the crystal size. By optimization of the hydrothermal synthesis, silicoaluminophosphate crystals with hexagonal rod-like morphology, large crystal size, and optical clearness have been obtained (16).

2. Size and Shape Control

Relatively defect-free microporous zeolite crystals and microporous aluminophosphates can result from hydrothermal synthesis (17). However, serious problems are encountered in the preparation of large synthetic molecular sieve crystals, although natural zeolites can occur as huge crystals. Many attempts (18,19) have been made to control the crystal size of molecular sieves, including novel routes for the crystallization of large single crystals from nonaqueous solution (20). Efforts were directed to obtaining large zeolite single crystals, narrow particle size distribution, and perfect morphology.

Large $AlPO_4$-5 crystals have been synthesized under conventional hydrothermal synthesis conditions, using triethylamine as template (21). Millimeter-sized $CrAPO_4$-5 and $MgAPO_4$-5 crystals with excellent morphology are obtained from concentrated gels containing HF (22). Very high-quality $AlPO_4$-5 crystals up to a length of 1.4 mm have been crystallized in a hydrothermal synthesis with a higher dilution of the synthesis gel and by replacing the template triethylamine with tripropylamine (23).

The optimization of hydrothermal synthesis parameters allowed the growth of mordenite and MFI crystals of several hundred micrometers (24) and the synthesis of large single crystals of zeolite Y with diameters up to 210–245 μm (25).

Silicalite-1 single crystals have been synthesized in the presence of benzene-1,2-diol with a perfect morphology and an appropriate size ranging from $9 \times 3 \times 2\ \mu m^3$ to $165 \times 30 \times 30\ \mu m^3$, depending on the content of benzene-1,2-diol in the reaction system. It was shown that a silicon–benzene-1,2-diol complex has been formed in the reaction system, which proved to be important for the synthesis of the zeolite single crystals. The concentration of benzene-1,2-diol can be used to control the morphology and the twinning of the well-shaped crystals (26).

Recently, the role of F^- and pyrocatechol as complexing agents for silicon and aluminum species in the hydrothermal synthesis of zeolites was investigated. The complexed species could be slowly hydrolized to the active species, which forms the preliminary structure unit of Si-O-Si or Si-O-Al via condensation reaction. Offretite single crystals, which show a better morphology and larger size than those synthesized without complexing agent, have been successfully prepared by this method (27). Experimental results from similar investigations with pyrocatechol in the synthesis of silica-sodalite showed that the crystals have a much larger size and better morphology than those synthesized in the absence of this reagent (28).

In addition to the study of the influence of conventional crystallization parameters, such as alkalinity, temperature, gel composition, aluminum source, and water content, the effect of using microwaves, centrifugation, ultrasonication, and microgravity was also explored. In a microwave synthesis, large hexagonal $AlPO_4$-5 crystals up to a length of 130 μm have been obtained. A further processing of the mother liquor resulted in batches free of byproducts. $AlPO_4$-5 single crystals with a narrow size distribution and perfect hexagonal morphology are shown in Fig. 1 (29,30).

The application of ultrasound in the crystallization process did not change the crystal size in the case of zeolite A. However, the morphology of crystals obtained was completely unusual (10).

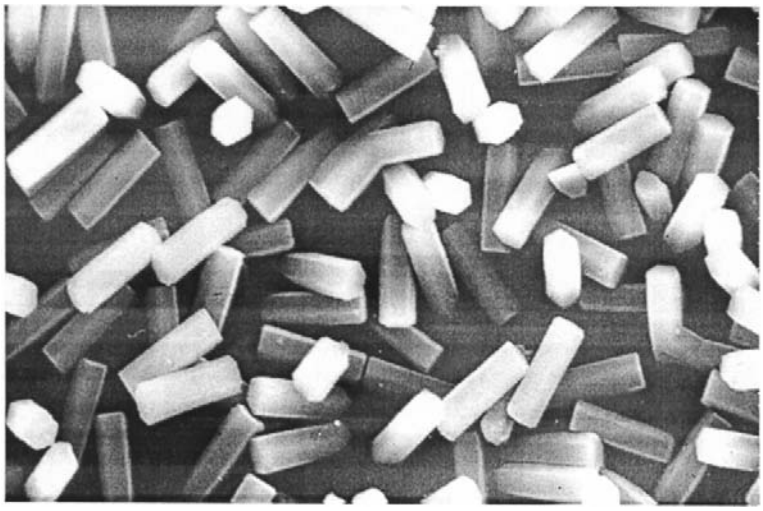

Fig. 1 Large, uniformly sized $AlPO_4$-5 crystals originating from a microwave-assisted crystallization. The standard gel composition optimized for microwave synthesis was 1.6 triethylamine:1.0 Al_2O_3:1.3 P_2O_5:1.3 HF:425 H_2O. No phase purifications have been applied. (From Ref. 29.)

A microgravity environment provides quite different conditions for zeolite crystal growth, including elimination of settling and convection, reduced collision breeding, and enhanced diffusion-limited growth. It was hypothesized that the microgravity environment in low earth orbit would minimize sedimentation, leading to the possibility of producing large zeolite crystals by allowing crystals a longer residence time in a high-concentration nutrient field. The microgravity environment should lead to zeolite crystals having a high degree of crystalline perfection with controlled defect concentration and location. With this intention, zeolite crystallization has been carried out under microgravity conditions (10^{-3}–10^{-6} g) on space shuttle missions. The different nucleation and growth history of zeolite A and X crystals in microgravity resulted in improved crystal morphology and an increase in crystal size, but they frequently led to different morphology in comparison with their terrestrial control samples (31). The high level of microporosity as well as the uniformity and symmetry of the orbit-grown crystals were attributed to a higher degree of crystalline perfection (32). The synthesis of high-silica ZSM-5 in microgravimetry resulted in crystals with intergrown and thus imperfect disk morphology up to 70 μm in diameter (33). However, very similar space-grown ZSM-5 materials showed a reduction in external surface area and activity, which is interesting for shape-selective catalysis (34).

B. Inclusion of Optically Functional Guest Molecules in Large Zeolitic Crystals

The examples described in the last section are different attempts to synthesize large well-shaped defect-free zeolites as host materials. However, photonic applications require additional modification of the crystals to realize optical functions. Guest/host arrangements have to be constructed by tuning the composition of the composites. The optical

functionality of guest/host materials is achieved by the incorporation of guest molecules, which are dispersed, organized, and protected by the molecular sieve framework. This can be carried out in different ways suited for special classes of dyes and concentration ranges without causing serious damage to the inorganic framework.

1. Crystallization Inclusion During Synthesis

The inclusion of functional guest species during synthesis is a way to obtain extraction-stable composite materials without performing any postsynthetic treatment (35,36). Organic molecules are added to the common synthesis gel. They can be included in the growing zeolite under the preconditions that (a) the organic molecule is soluble in the synthesis gel, (b) it is stable under the pH and temperature conditions of the hydrothermal synthesis, and (c) it does not disturb the zeolite synthesis. Many positive examples have been found, where the molecule was either a cation or had a proton-accepting group. Using the crystallization inclusion method, metal complexes and cationic organic dyes such as methylene blue (37,38), phthalocyanines (39–41), as well as rhodamine dyes (42) have been occluded in molecular sieves of the AFI and FAU type. The method is not limited to cationic species; the neutral molecule thioindigo (43) was included in zeolite NaX by adding the dye to the structure-directing template. This extensively investigated method has also been expanded to crystallization inclusion of some unstable chromophores like coumarine and azobenzene dyes by microwave techniques taking advantage of the mild synthesis conditions and a short crystallization time (44).

The conventional and microwave-assisted synthesis of composites consisting of rhodamine BE50 encapsulated in large $AlPO_4$-5 crystals was reported. Since the molecules with dimensions of 0.91×1.36 nm^2 are too large to fit into the 0.73-nm-wide pores of the $AlPO_4$-5 host, the dye molecules are located in cavities that have been formed around them. The accommodation of the rhodamine dye up to a concentration of 1.3×10^{-2} molecules per unit cell in defect sites of the host crystal seems to be without negative consequences for the morphology of the crystals that are large enough for optical applications (42).

Incorporation of a dye into the pores has been successfully achieved by using conventional hydrothermal synthesis where guest molecules replaced template molecules without framework destruction. The linear dye molecule pyridine-2 with a diameter of 0.63 nm fits excellently into the $AlPO_4$-5 pores, resulting in an ordered material where the dye molecules are aligned along the crystallographic z axis. Depending on the dye content, composite crystals with a length up to 100 μm and different crystal morphologies have been observed (45).

2. Postsynthetic Treatments

Postsynthetic treatments, such as (a) ion exchange, (b) in situ guest synthesis, and (c) adsorption from gas or liquid phase, allow the insertion of guests into the pores of large zeolite single crystals. A precondition for the postsynthetic introduction of guest molecules is mostly the calcination of the zeolitic material, which is necessary to remove structure-directing organic template molecules that have been incorporated during synthesis. This thermal treatment can cause partial destruction and unspecific disruption of the inorganic framework, especially in case of large crystals (46).

a. Ion Exchange

Cations that compensate the framework charge of non-neutral zeolites can be exchanged with aqueous solutions (47). Ion-exchange of small monoatomic cations have been studied

extensively, especially with regard to applications in detergents (48). The process can also be used for the introduction of large cationic chromophores, e.g., methylene blue, into NaY (37,49). Composite materials consisting of 3-μm crystals of zeolite L and pyronine, oxonine, or resorufin have been obtained by ion exchange from aqueous solution (50,52).

As a result of kinetic investigations of the incorporation of cationic dyes in zeolite L, the ion exchange has been described as an equilibration process, where the ion-exchange capacity controls the species concentration in molecular sieve channels (51–53). Attempts with ion exchange from nonaqueous solutions have not been successful up to now (54).

b. In Situ Guest Synthesis

The in situ synthesis of organic dyes and complexes (55) is a way to incorporate chromophores that decompose under the hydrothermal conditions of the crystallization inclusion. "Ship-in-the-bottle" anchoring is the special case of in situ synthesis where the guest molecule is too large to enter the pore system of molecular sieves. Generally, in situ synthesis results in an irreversible fixation of guest molecules via steric constraints of the host material, as was shown for the in situ synthesis of Nile Red in a silica-rich zeolite Y, resulting in a material with a dye concentration of 0.05 molecule per supercage (56). The method also allows the synthesis of unstable neutral azo dyes and zwitterionic methyl orange within negatively charged faujasite NaY (57). A ship-in-the-bottle synthesis of spiropyrans inside the supercages of NaY was carried out by an intrazeolitic condensation reaction (58).

There has also been a growing interest in encapsulation of polymers within inorganic host materials like zeolites, mesoporous silica, or silica nanotubes. The resulting hybrid materials offer the possibility to study optical and electrical properties of individual polymer chains or to prepare conducting chains as "molecular wires." Polymerization in zeolite channels (59,60) was carried out in situ with aniline (61,62), pyrrole derivatives (63), and with vinyl ether (cationic polymerization) in pores of HY to produce novel hybrid materials (64). The oligomerization of ethene in large (150 μm) crystals of HZSM-5 has also been shown (65).

c. Adsorption

Organic molecules can be inserted by adsorption from the vapor phase or solution into microporous voids (41,66–69). Only molecules with dimensions that fit to the pores of molecular sieves can be occluded. In order to prevent coadsorption of the solvent during adsorption from the liquid phase, the sterically demanding 1,3,5-triisopropylbenzene was used as a solvent that is too large to enter the pore system itself (70). By this method, many dyes, e.g., donor–acceptor substituted azo dyes (71), have been incorporated in $AlPO_4$-5 single crystals.

However, gas phase inclusion should be preferred as a clean method if guest species are of interest, which can be evaporated. The preparation of composite materials consisting of large crystals of zeolites and neutral dyes like azobenzene (86) as well as biphenyl or *p*-terphenyl (72) were performed by gas phase reaction of the dehydrated host with the guest molecules. Polar donor–acceptor substituted dyes (73) have also been successfully incorporated in single crystals of $AlPO_4$-5, ZSM-5, silicalite-1, zeolite X and Y by using the same method.

Guest/host composites consisting of organic acids (benzoic, salicylic and acetylsalicylic acid) and VPI-5 have been obtained by adsorption from a supercritical CO_2 solution. Some of the problems found in conventional adsorption processes can be overcome by using the supercritical fluid technique (74).

III. OPTICAL CHARACTERIZATION OF LARGE COMPOSITE CRYSTALS

A. Microscopy with Polarized Light

The simplest method for the investigation of zeolitic composites is the visual inspection of crystals by means of microscopy. The color of the crystals is a sensitive indicator for the incorporation of guest species. Inhomogeneities in the color often indicate diffusion barriers or crystalline imperfections. Chromophore-loaded zeolite crystals often show nearly the same color as the nonencapsulated solid dye, but sometimes also drastic color changes can be observed, indicating a host influence on the dye.

Using linearly polarized light, one can obtain information about the alignment of guest molecules in the restricted geometry of the host lattice. Anisotropic light absorption

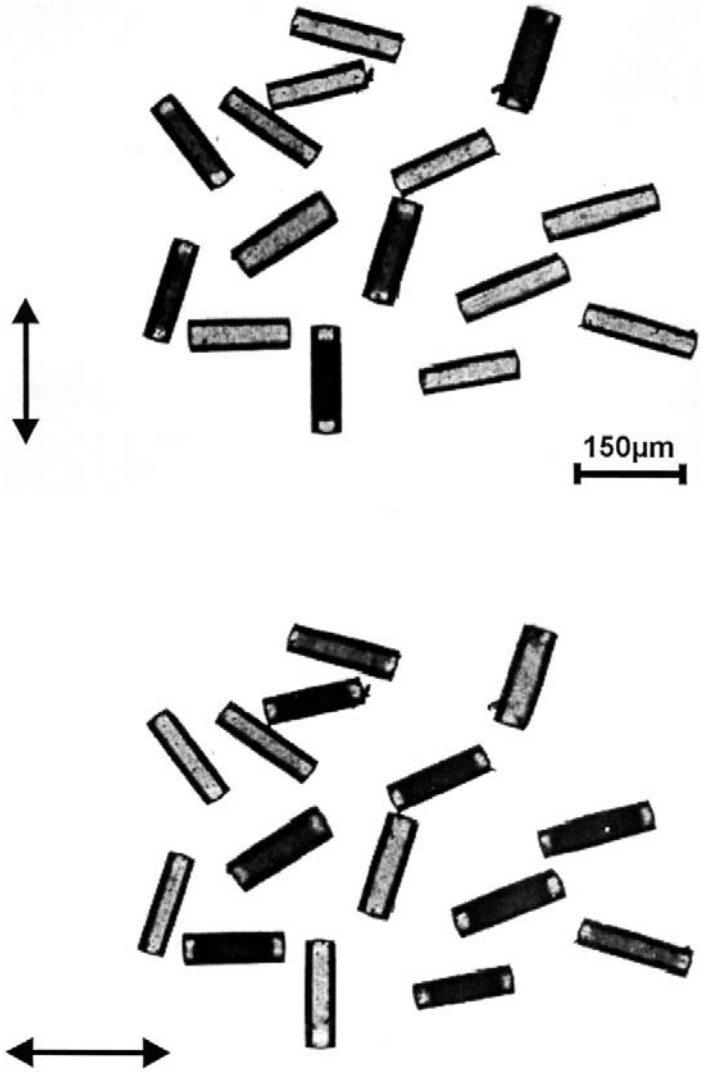

Fig. 2 Microscopic picture of $AlPO_4$-5 crystals loaded with p-nitro-aniline pNA in transmission with polarized light. The direction of the polarization plane is indicated by arrows. (From Ref. 69.)

or linear dichroism becomes visible by polarization-dependent observation of composite crystals as shown in Fig. 2 (75). If the dipole moment of the electronic transition of incorporated molecules and the electric field vector of the polarized light are parallel, the crystals absorb light strongly, resulting in a dark color. Otherwise the crystals show little or no coloration depending on the degree of alignment of the guest molecules. These effects are specific signs for guest incorporation within the host, in contrast to the adsorption of molecules on outer surfaces.

Perfectly ordered chromophores can be found in zeolite crystals as was shown for rod-like molecules in the one-dimensional channel system of $AlPO_4$-5 (75) or for cobalticinium metal–organic complexes in a nonasil framework (76). These crystals appear as small polarizers that could be applicable in optical microdevices.

The homogenous distribution of the coloring species in red-brown, selenium-doped cancrinite can also be observed by polarization microscopy. Selenium ions have been introduced into a cancrinite matrix forming large, uniform, hexagonal crystals of good optical quality. If the crystals are observed in a transmission microscope using polarized light, the crystals appear red or yellow for parallel or perpendicular alignment of the polarization plane relative to the crystal's long axis, respectively (77).

The isomorphous substitution of Co^{II} for Al^{III} in large hexagonal $AlPO_4$-5 crystals of excellent optical quality also reveals an interesting visual result. The cobalt blue CoAPO-5 crystals aligned parallel to the polarization plane look turquoise while the crystals perpendicular to this plane appear red. This has been assigned to structure-related distortions of the $[Co^{II}O_{4/2}]$ tetrahedra (78,79).

Using two crossed polarizers, birefringent properties of dye-loaded molecular sieve crystals can be visualized. The birefringence mainly results from the ordering of the molecules by the pores of the microporous host. The crystals appear in artificial colors due to the interference of the ordinary and the extraordinary light waves which pass the crystal with different phase velocities. Since the birefringence is strongly controlled by the guest species, this effect can be used to probe the distribution of adsorbates over the crystals (75,80).

In summary, visual microscopic investigations on zeolitic guest/host composites are a simple but sensitive method (a) to find the correlation between crystals shape and the direction of molecular sieve pores, (b) to check the alignment of guest molecules within molecular sieve pores, or (c) to investigate a structure-related symmetry distortion of coloring inorganic species and (d) to probe the distribution of guest molecules throughout the crystal.

B. UV/Vis Spectroscopy on Individual Zeolite Crystals

Since developments in the field of zeolite-based advanced materials critically depend on improved analytical methods for the characterization of large zeolite composite crystals (81), useful spectroscopic techniques have been adapted to the study of zeolitic guest/host materials and intrazeolite chemistry.

The quantification of the anisotropic light absorption is provided by polarization-dependent UV/vis spectroscopy on large individual molecular sieve crystals. The absorption bands correspond to optical transitions between electronic states of organic molecules, which are strongly dependent on the structure, geometry, and symmetry of the optically functional unit, e.g., of the dye molecules. Since both the orientation and the electronic states of included guests are important for advanced optical applications of guest/host composites, polarization-dependent absorption and fluorescence spectra of

microcrystals can provide valuable information on the electronic states, on the alignment and intermolecular interactions of included functional molecules, on the influence of the environment, and on the concentration of zeolite encapsulated organic species (68, 69,73).

The optical anisotropy, caused by the alignment of adsorbed organic molecules constrained by molecular sieve pores, can be studied quantitatively (Fig. 3) by means of UV/vis spectroscopy on large crystals. It turned out that this method is especially suitable for systems with low chromophore concentration (82).

Micro-optical absorption spectroscopy has also been reported for BiI_3 molecules incorporated into channels of mordenite and $AlPO_4$-5 single crystals. Based on polarized absorption spectra, the molecular shape, the location, and the orientation of the guest species have been discussed. In mordenite, the molecular axis of the BiI_3 molecules can be oriented with respect to the molecular sieve channel. Since the polarized absorption spectra in neutral $AlPO_4$-5 show no dependence on the channel direction, the importance of the cations for the orientation of the adsorbed molecules seems to be indicated (83).

The application of the method to inorganic chromophore-zeolite composites has also been demonstrated in studies on selenium-loaded mordenite (84) and cancrinite (77), where the absorption spectra strongly depend on the orientation of the zeolite crystals with regard to the polarization of the observation light. The polarized absorption of selenium-containing cancrinite single crystals reflects the visual findings of microscopic observations. Different bands at 290 and 430 nm, attributed to the Se_2^{2-} dianions, and strongly polarization-dependent bands at 350 and 510 nm, belonging to the Se_2^{-} radical anions, have been found in the absorption spectra (82).

For Co^{2+} and Cr^{3+} in large $AlPO_4$-5 crystals a polarization-dependent absorption has been observed, indicating an anisotropic coordination of the coloring species distorted by the molecular sieve structure (46,78).

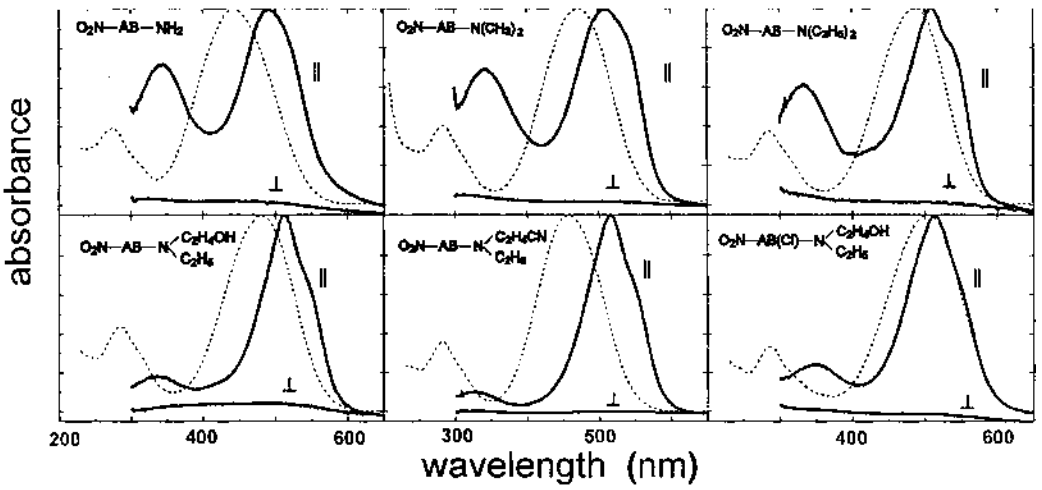

Fig. 3 Polarization-dependent absorbance of highly ordered arrangements of azo dyes in $AlPO_4$-5. The polarization of light parallel or perpendicular to the hexagonal $AlPO_4$-5 z axis is indicated by ∥ and ⊥, respectively. The spectra of dyes in ethanol are given for comparison. (Adapted from Ref. 71.)

C. Refractive Index and Birefringence

An application of new materials requires detailed knowledge of relevant material parameters related to the type of application. For optical devices, the refractive index is of crucial interest. The design of photonic materials can only be successful if this decisive material parameter can also be controlled. For example, exact relations between the refractive indices are required to achieve an efficient frequency conversion process in nonlinear optical applications.

Most of the methods commonly used to obtain the refractive index cannot be applied due to the size of molecular sieve host. Recently, a method (70) has been presented for the determination of the refractive index of dye-loaded molecular sieve crystals intended for use in optical applications. The method developed for microcrystals is very similar to the well-known prism method for the determination of the refractive index. The microcrystal prism method uses the deflection of a light beam by microcrystals and delivers the wavelength-dependent values for the refractive index. In unloaded samples of $AlPO_4$-5 molecular sieves, the birefringence (the difference of refractive indices for different polarizations) is very small, but it is drastically enhanced in dye-loaded samples. The strong anisotropy of the refractive index is a direct result of the alignment of molecules. This effect offers the possibility to control the birefringence of zeolitic optical guest/host materials by varying the degree of loading. Therefore, refractive indices of guest/host systems can be tuned in order to meet very special requirements, e.g., for frequency conversion applications. The microcrystal prism method can be applied to any well-shaped crystal with known geometry. It has already been used for $AlPO_4$-5- and ZSM-5-based nanocomposites and for metallo-organic crystals (85).

By measuring the transmittance between two polarizers, one can also determine the birefringence of large well-shaped single crystals of zeolitic guest/host materials (Fig. 4) (86). The ordinary and the extraordinary light waves pass the crystal with different velocities and interfere with each other. This interference results in the oscillatory behavior of the transmittance. The transmittance of the crystal depends on the phase shift between the two light waves. If the crystal with thickness L is placed between two parallel polarizers forming an angle α with the crystal axis, the phase shift δ results in a transmittance $T_\alpha^\parallel$ given by

$$T_\alpha^\parallel = T_{\text{sample}} - \frac{\Delta T_\alpha}{2}(1 - \cos\delta) \tag{1}$$

where the values T_{sample} and ΔT_α can be determined from the extrema in the spectral behavior of the birefringence. The phase shift is connected with the birefringence $n' = n_e - n_o$ by

$$\delta = 2\pi L n'/\lambda \tag{2}$$

This method has been applied to the determination of the birefringence of AFI- and MFI-based composites and allows a determination of the birefringence with an accuracy of 10^{-3} (86).

D. Infrared Spectroscopy

From the study of infrared (IR) radiation characteristically absorbed by molecules, one can obtain useful analytical information about vibrational and rotational states of molecular species. Polarized IR spectroscopy can be used for the assignment of the IR bands to certain vibrations in molecules or for the analysis of the orientation of molecules using the

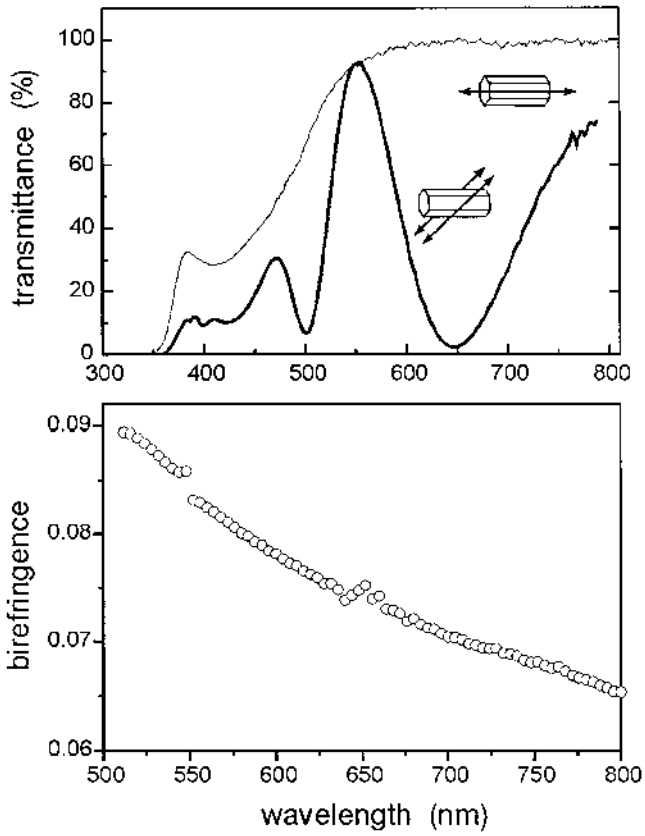

Fig. 4 Birefringence of an azobenzene-loaded $AlPO_4$-5 crystal. Top: Determination of the birefringence from the oscillatory behavior of the transmittance of a 13-μm-thick crystal investigated between two parallel polarizers (thick line). Normal transmittance of the same crystal observed with a polarization parallel to the crystal's *z* axis is given for comparison (thin line). Bottom: The wavelength-dependent birefringence calculated from the transmittance measurements.

dichroic ratios. Polarized Fourier transform infrared (FTIR) microscopy on individual zeolite crystals has been used for determining the orientation of the adsorbate molecules in zeolite pores such as *p*-xylene-loaded single crystals of silicalite-1. Since the vibrational modes of para-substituted benzenes are well known, the analysis of the polarization dependence of characteristic absorption bands leads directly to information about the orientation of the guest molecules with respect to the channel structure (87).

The orientation of molecules interacting with Brønsted or Lewis acid sites were also analyzed by polarized IR absorption of benzene, acetonitrile, and pyridine within large crystals of SAPO-5 and GaPO-5 (88). Apart from information on the orientation of guest molecules, the determination of the strength of intermolecular H bonding is accessible by means of IR microspectroscopy. Using this method it has been demonstrated that H bonding between *p*-nitroaniline (pNA) molecules adsorbed in $AlPO_4$-5 crystals depends strongly on loading and temperature, while they are always aligned fairly parallel to the channel direction of the molecular sieve (89). Molecular vibrations with a transition moment parallel to the long axis of the pNA such as symmetrical stretching vibrations are

mainly excited by radiation polarized parallel to the long axis of the $AlPO_4$-5 crystal. Therefore, it can be concluded that the molecules are oriented parallel to the channel axis. The dichroic ratio d of the bands

$$d = I_{\parallel} / I_{\perp} \tag{3}$$

can be used to calculate a mean tilting angle of molecules with respect to the channel axis using the formula

$$\theta = arctan(2/d)^{1/2} \tag{4}$$

For the composite system pNA adsorbed in the one-dimensional pore system of $AlPO_4$-5, a mean deviation from the crystal's long axis of about 12° can be inferred from the dichroic ratio of the symmetrical NH_2 streching band of the pNA guest molecules at 3392 cm^{-1} (89).

In situ FTIR microscopic investigation of large single crystals of AFI molecular sieves has also provided a direct spectroscopic evidence for the existence of Brønsted acid sites (90). A microscope FTIR mapping method (91) has been used for studying intrazeolitic anisotropic diffusion processes of hydrocarbon molecules in single silicalite particles. This method is based on the determination of the adsorbate concentration profiles by spatial measurements of the IR absorbance.

E. Raman Spectroscopy

Like IR absorption bands, the frequencies of the Raman-active vibrations and their intensities are characteristics of the various groups and linkages in molecules. Furthermore, polarized Raman scattering investigations are a powerful method to check alignment and interactions of guests molecules and to gain information about intermolecular structures, such as hydrogen bonds. For the ordered systems expected in the case of zeolite-encapsulated species, one can obtain different Raman spectra depending on the polarization configuration between incident and scattered light with respect to the sample (Fig. 5). From these investigations, one can identify the alignment of the Raman-active vibrations in addition to their frequencies and intensities.

For example, the alignment and different physical states of pNA adsorbed in large crystals of $AlPO_4$-5 has been investigated by this method (92). The Raman spectra are characterized by intensive broad background of the zeolitic matrix and some pronounced bands arising from the guest molecules. Since the pNA molecules have only one relevant electronic transition polarized parallel to the molecular axis in the visible spectral region, polarization effects are to be expected. Strong Raman bands of the adsorbate were obtained for a polarization of the incident and scattered light parallel to each other and parallel to the crystal's long axis only. This indicates an excellent alignment of the included molecules. Comparing the arrangement of pNA in the straight pores of $AlPO_4$-5 with the results of Raman spectroscopy of solid pNA, it was concluded that pNA forms dipole chains with intermolecular hydrogen bonds in both systems. In the solid, the antiparallel and S-shaped arrangement of the dipole chains causes a total polarization of zero, whereas in the channels of $AlPO_4$-5 all dipole chains point in the same direction. The noncentrosymmetrical arrangement results in second-order nonlinear optical effects (see Sec. IV).

Polarized Raman scattering has also been successfully applied to show the stabilization of one-dimensional selenium chains within mordenite and cancrinite (93) as well as in $AlPO_4$-5 (94). Helical Se chains as well as Se_6 or Se_8 ring molecules were formed in mordenite (95) and in $AlPO_4$-5 single crystals with a size up to 50 × 150 μm (96).

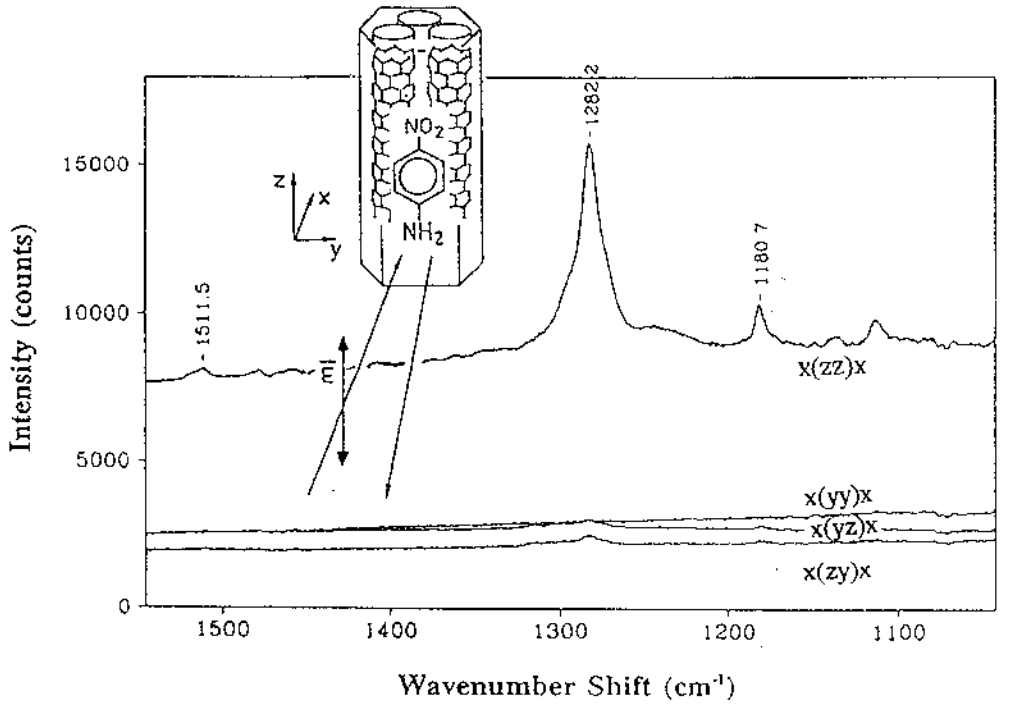

Fig. 5 Raman spectra of pNA in $AlPO_4$-5 for different polarizations. Strong Raman bands from the adsorbed pNA were only obtained for excitation with light polarized along the crystal axis (z direction) and for the detection of scattered light with the same polarization. (From Ref. 80.)

IV. OPTICAL APPLICATIONS BASED ON ZEOLITIC GUEST/HOST MATERIALS

The optical functions of zeolite-based materials are determined on different length scales. In the subnanometer range, the electronic states of encapsulated guest atoms or molecules determine the interaction with photons. On the nanometer scale, functional guest molecules can be organized and oriented by inclusion in cavities or channels of the zeolite framework. On the micrometer scale, the optical quality of the zeolitic host controls the propagation of light, e.g., scattering and diffraction phenomena. Progress in the synthesis of large zeolite crystals and independent tuning possibilities on every length scale involved in optical processes allow an efficient design of optical materials.

However, in optical applications of composite materials containing organic parts, the photophysical and photochemical stability plays a critical role. Because of insufficient reliability, these materials have not been considered for photonic application up to now. The lack in photostability leads to a mostly irreversible photobleaching process in which organic molecules undergo a chemical decomposition upon absorption of light. Photobleaching can be characterized by a quantum yield of photobleaching ϕ_b, which is defined by the number of bleached molecules (N_b) divided by the number of photons absorbed (N_γ) during in a fixed time interval: $\phi_b = N_b/N_\gamma$. The complex mechanisms of photobleaching sometimes involve species from the surroundings, frequently oxygen. The oxidative attack on dyes by highly reactive photogenerated singlet oxygen is a very important reaction that may lead to photobleaching (97). Many attempts have been

made to increase the photostability of organic molecules in matrices, e.g., by variation of the oxygen concentration, by addition of a protective agent, or by encapsulation of the organic molecules. However, the stabilization of adsorbed dye molecules by rigid hosts such as zeolites against photobleaching and other influences is still under discussion (4,35,98–100).

Enhanced photostability has been obtained by encapsulation of rhodamine B molecules in solid xerogel matrices (98). It has also been stated that encapsulation should stabilize $Ru(bpy)_3^{2+}$ against irradiation, but the incorporation in supercages of zeolite Y has not led to a noticeable decrease in photodecomposition as compared with an aqueous solution (99). On the other hand, an enhanced photostability by incorporation of dye molecules into molecular sieves has been reported. This effect can probably assigned to a deactivation of the singlet oxygen $^1O_2$ to the normal triplet oxygen $^3O_2$ by the surrounding molecular sieve host (4). The photostability of porphyrin incorporated in $AlPO_4$-5 exceeds that of porphyrins adsorbed at the outer $AlPO_4$-5 surface by one order of magnitude (35). The 1,6-diphenyl-1,3,5-hexatriene molecule is reported to be stable after insertion into zeolite L, although it is very photolabile in solution (100). These results, indicating an improved chemical and photochemical stability, make the encapsulation of organic molecules in zeolite channels a promising strategy for the design of new zeolite-based materials.

A. Optical Sensing

A sensor is a device that responds to a physical stimulus or to a change in chemical concentration by converting it to a measurable quantity. Sensors are especially useful for in situ measurements in industrial processes or medical applications. They should have a number of qualities such as sensitivity, specificity, selectivity, capability of detection in a multicomponent environment, and a long lifetime. In optical chemical sensors, the analyte is recognized because it changes optical properties such as light intensity, luminescence decay time, spectral position of emission maxima, or polarization of light as a function of the analyte concentration.

Zeolitic guest/host materials have now been investigated for the use in chemical sensors because of their high surface-to-mass ratio, their selectivity, as well as their temperature and long-term stability. Especially for gas phase sensor applications, the highly porous zeolites are ideal sensor materials, since they provide good contact with the gas stream. The progress in the oriented growth of zeolite films (101–103), as well as the recently developed transparent zeolite films (12,13,104) and silicon wafers with spatially ordered zeolite particles (105) have enlarged the possibilities for application (106).

An optical organic-vapor sensor has been designed by inclusion of the highly solvatochromic dye Nile red within the nanopores of zeolite Y (107). In the presence of various organic molecules, Nile red exhibits wavelength shifts in both absorbance and fluorescence bands. Restriction of the dye molecule in the zeolite pores results in a high selectivity by combining the shape selectivity of the inorganic host with the chemical sensitivity of the solvatochromic guest species.

The efficient luminescence quenching properties of a zeolite-encapsulated ruthenium(II) bipyridyl complex ($Ru^{2+}(bpy)_3$) by oxygen has been used for the development of an optical sensor with special properties. The crystalline inorganic matrix of zeolite Y incorporated into silicon polymers provides good long-term stability, fast response time to oxygen, high quenching efficiency, and a unique sensitivity of the novel zeolite-based oxygen sensor material (108). A high-temperature fiberoptic gas sensor has been developed

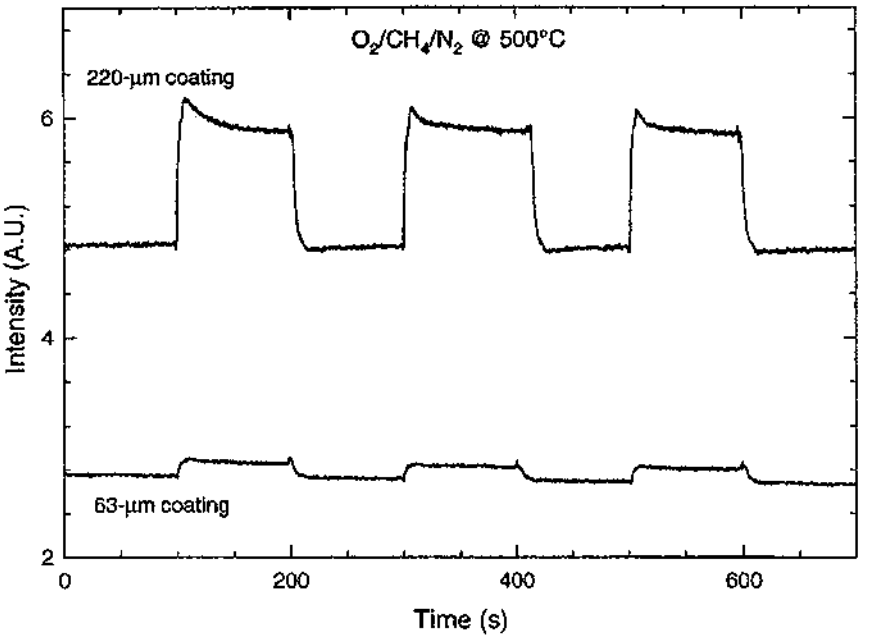

Fig. 6 Fluorescence response of a fiberoptic sensor at 500°C. The end of a 440-μm-thick silica fiber was coated with silica-encapsulated Cu:ZSM-5 and excited with blue or UV light. Devices with different thicknesses of the sensitive material were tested in gas mixtures of oxygen and various reductants. Here the oxygen content is switched between 3000 ppm and 300 ppm at 100-s intervals. (From Ref. 109.)

with copper-exchanged zeolite Cu:ZSM-5 showing fluorescence quenching in the presence of oxygen. The quenching mechanism involves the rapid and reversible conversion of strongly fluorescent cuprous Cu^{1+} ions to nonfluorescent Cu^{2+} ions. The fluorescence intensity being proportional to the Cu^{1+} concentration was, therefore, directly dependent on the oxygen content in the analyte (Fig. 6). The Cu:ZSM-5 fluorescence indicator was bonded onto the end of a silica optical fiber, employing sol-gel-processed silica as a binder. As a result of this development, a solid-state high-temperature oxygen-sensitive device with a silica-encapsulated Cu:ZSM-5 sensor element is feasible as shown in Fig. 6 (109).

Microdevices such as chemical sensors are also suitable for laboratory-on-a-chip applications (110,111). Zeolites with their high adsorption capacity can enhance the sensitivity of microscaled sensor devices. For example, the application of ultrathin LTA-type films grown on piezoelectric devices for humidity sensing has been proposed (103). Similarily, a novel MFI-based chemical sensor has been developed by combining the high sensitivity of micromechanical cantilevers commonly used for atomic force microscopy with the excellent adsorption properties of microporous single crystals. The miniaturized device operates as a humidity sensor probing the increase in weight of a few microcrystals due to water adsorption in the nanogram range (112).

B. Light Harvesting

The primary processes of natural photosynthesis consist of the photon absorption by the light harvesting complex (LHC), the ultrafast energy transfer, and the trapping in the

reaction center where the conversion of solar energy into chemical energy takes place. It is remarkable that the absorption process and the conversion of the excitation energy into chemical energy are spatially separated from each other. A larger number of antenna pigments provide an increase in the overall cross-section for light absorption, they harvest the sunlight and channel photons via a rapid energy transfer to a reaction center. The collection of light energy by many pigments and the transfer to one reaction center is the so-called antenna effect. This antenna effect has also been studied in artificial systems. The interest in these studies is not only to provide a better understanding of the light harvesting step but also to design artificial devices for solar energy conversion (113).

Organized dye molecules in the channels of zeolite microcrystals provide very promising possibilities to form an artificial antenna device (114–116). The well-defined spatial arrangement of guest molecules in cages and channels of crystalline zeolites results in molecular assemblies which additionally promote the stabilization of photochemically generated redox pairs. The possibility for intrazeolitic long-lived charge separation has been demonstrated, for example, in zeolite L (117) and in faujasites (118,119).

Cationic dye molecules entrapped in the channels of large crystals of zeolite L by an ion-exchange process have also been used as light-harvesting systems (Fig. 7) (120). The restricted geometry of the zeolite pores prevents dye aggregation and self-quenching even at high dye concentrations. The occurrence of energy transfer has been proven by

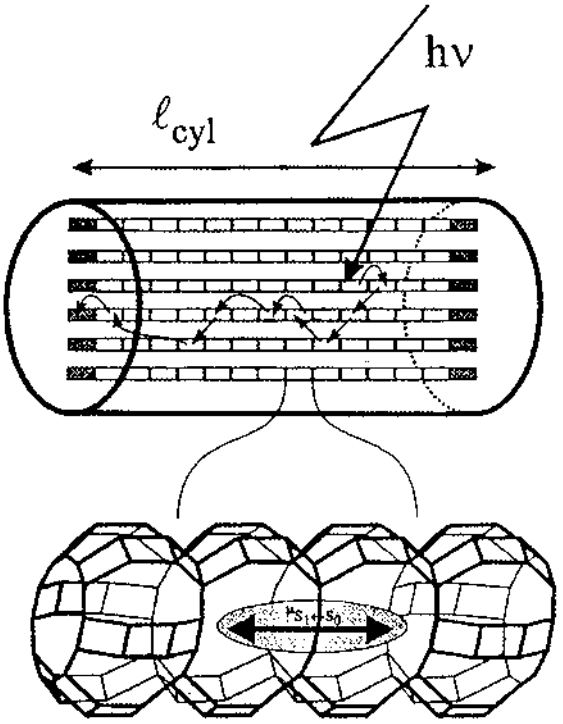

Fig. 7 Schematic picture of a zeolite L–based artificial antenna system for light harvesting. The light is absorbed by organized organic guest molecules acting as donors (empty rectangles) and transported by energy migration to an acceptor acting as a specific trap (dark rectangles). The bottom detail shows a dye molecule, with its electronic transition moment aligned with respect to the channel axis of zeolite L. (From Ref. 121.)

simultaneous incorporation of two different fluorescent dye molecules—pyronine and oxonine—using fluorescence spectroscopy of zeolite suspensions or fluorescence microscopy on large zeolite L single crystals (72). After excitation of pyronine molecules at 470 nm, the fluorescence emission of both pyronine and oxonine has been observed, demonstrating an intrazeolitic energy transfer.

The efficient light-harvesting nanocrystals of dye-loaded zeolite L showing extremely fast energy migration may have great potential for the development of a new type of thin-layer solar cell in which the absorption of light and the creation of an electron-hole pair are spatially separated, as has been known from the natural photosynthesis process (121).

C. Lasing

A laser medium can amplify light by stimulated emission. Incorporation of such a medium into a resonator results in a laser that has a highly monochromatic and coherent output. The properties of laser light offer applications ranging from spectroscopy to material science or communication technology. Microlasers and microresonators are of considerable interest in device technology for miniaturization reasons and because interesting properties result from the reduction of the laser dimensions.

Attempts have also been made to develop solid-state lasers based on organic dye compounds. Zeolitic guest/host systems are one example of these developments leading to new microlasers. They have been based on strongly fluorescent guest molecules, e.g., pyridine-2 (122) or rhodamine BE50 (123), incorporated into $AlPO_4$-5 microcrystals.

The properties of a microlaser depend on its gain, efficiency, thermal sensitivity, photochemical stability, and scattering losses, but also on size and shape of the microresonator. Since the zeolite host crystal forms a hexagonal micrometer-sized prism, a naturally grown microresonator supporting a so-called whispering gallery mode has been realized (Fig. 8). The large number of laser-active organic molecules that could be incorporated in the molecular sieves may result in different systems with laser properties, covering the whole visible spectral region. In addition, the light generation efficiency could be increased in these microlasers since the spontaneous emission rate is modified by the confinement of the modes in a small volume. The photon confinement in a microresonator and scattering phenomena induce interesting effects recently reviewed in detail by Laeri et al. (124).

Zeolitic guest/host systems combine organic laser-active media and crystalline, inorganic, hexagonal microresonators into a micrometer-sized laser material which is of interest for micro-optoelectronic devices.

D. Frequency Conversion

In addition to the alignment of molecules, an interesting phenomenon occurs for dipolar molecules adsorbed in pores of molecular sieves. It was found (67,125–128) that these molecules show a preferred dipolar orientation in the pores resulting in large polar domains. This noncentrosymmetrical arrangement of molecules resulting in a macroscopic dipole moment is an unique phenomenon with remarkable physical implications. The most important of them are the nonlinear optical properties. They are caused by the nonlinear behavior of the polarization, which has second-order effects in polar systems.

Usually, light waves do not interact with each other and the medium shows linear optical behavior. Mathematically this is described by a linear relation of the polarization P of the medium with the electric field strength E,

$$P = \chi^{(1)} E$$

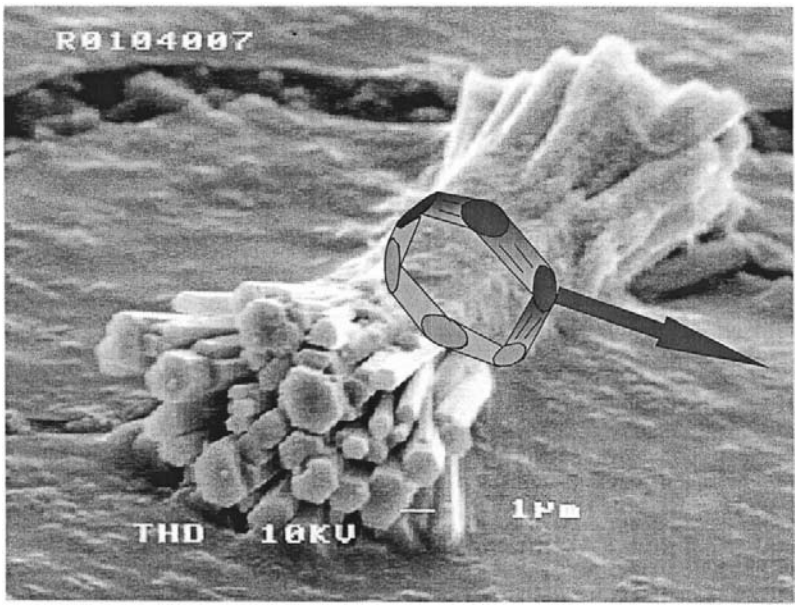

Fig. 8 SEM picture of a pyridine-2/$AlPO_4$-5 microcrystal bundle with laser properties. The middle section forms the optical resonator by total internal reflection at the side faces inside the hexagonal prism (whispering gallery mode). (From Ref. 122.)

which is valid at low light intensities. Here $\chi^{(1)}$ is the (first-order) susceptibility of the medium. At higher light intensities, deviations from this behavior occur and lead to a nonlinear response of the medium. This is described by additional terms in the power expansion which can be related to higher order nonlinear optical effects.

$$P = \chi^{(1)}E + \chi^{(2)}EE + \chi^{(3)}EEE + \cdots \tag{5}$$

Here $\chi^{(n)}$ are the higher order susceptibilities. The second-order effects are the strongest nonlinear effects and, therefore, the most important ones. Electro-optical switches and frequency converters can be constructed on the basis of these effects. Second-harmonic generation (SHG), which is also related to the second-order susceptibility $\chi^{(2)}$, also has some importance for applications but its most valuable properties are easy detectability and suitability for material characterization.

Molecular sieve powders containing organic guest molecules were investigated by SHG. Surprisingly, it was found that most of these composites show rather strong nonlinear optical (NLO) effects (67). It became clear from these experiments that polar domains of dipole molecules were formed, but the origin of these polar arrangements could not be clarified and has been a matter of discussion up to now. The most probable mechanism for the formation of the polar arrangements is the ordering of the molecules into polar chains during the entrance process into the molecular sieve channels (125–127). This mechanism is consistent with the pyroelectric studies on these materials, which revealed the size of the polar domains (128,129).

Better insight into the NLO properties was gained by using large dye-loaded single crystals allowing polarization-dependent detection of the frequency-doubled

radiation (125). It was possible to determine the different nonlinear susceptibility tensor components that contain the detailed NLO parameters of the material. It was found for pNA-based composites that the frequency-doubled radiation is polarized parallel to the direction of the straight channels (e.g., in $AlPO_4$-5) (125,126). Furthermore, the second harmonic can only be generated if the exciting light wave has a polarization parallel to the same axis. This means that the nonlinear susceptibility tensor is dominated by one component (χ_{zzz}) only, or, in other words, that only waves polarized parallel to the channel direction can interact with each other. It was recognized, however, that it is impossible for such a material to fulfill a so-called phase-matching condition. Phase matching is a condition for the refractive indices of the NLO material and a prerequisite for any technical useful frequency-doubling material. To turn the dye-loaded zeolites into materials that could be of practical usefulness, it is necessary to tune the different tensor components in order to fulfill these conditions.

It can be shown that the NLO properties are determined by the direction and strength of the electronic transitions in the UV/vis region (126). These transitions are predominantly controlled by the guest molecules if a transparent host material is used. Very often, the optical behavior of the guest molecules can be described by a very low number (2 or 3) of electronic levels. Furthermore, the geometrical arrangement of these few-level systems is of importance. Unfortunately, pNA forms perfectly aligned electronic two-level systems in $AlPO_4$-5. Since all the electronic transitions are aligned parallel to one axis, only the electric fields parallel to this axis have a role in the NLO processes. Therefore, these materials seem useless for frequency conversion applications.

In contrary, dimethylaminobenzonitrile (DMABN) represents an electronic three-level system. Therefore, composites of DMABN and $AlPO_4$-5 behave very differently toward pNA/$AlPO_4$-5 as shown in Fig. 9 (126). Here the generated second harmonic radiation is not linearly polarized any longer. When the SHG polarized perpendicular to the axis is analyzed, the maximal SHG occurs at an angle of 45° between the polarization of the incident light and the crystal's long axis. When the SHG polarized parallel to the crystal axis is detected, a maximum of the SHG is obtained for a parallel polarization of the incident light, as for the pNA-based composites. It is obvious that different components of the susceptibility tensor are responsible for the different SHG signals here. These components result from different electronic transitions in DMABN in the visible region which show different orientations of the transition dipole moment in the molecule. In this guest/host system it is, therefore, possible to mix waves of different polarizations. This fact is an important precondition for the realization of phase matching in this material and, therefore, for efficient wavelength conversion.

Besides the electronic states, the geometrical arrangement can also be used to tune the tensor elements. For example, it has been shown that pNA forms zig-zag chains in silicalite-1. This composite shows tensor components different from χ_{zzz} as well (127).

A large number of composites of molecular sieves, such as $AlPO_4$-5, $AlPO_4$-11, VPI-5, ZSM-5, and dipole molecules, such as pNA, DMABN, and others, have been investigated. The polar orientation of the dyes in channels has been found in most of these systems, which could be the basis for the construction of NLO materials consisting of molecular sieves and organic molecules. The magnitudes of the $\chi^{(2)}$ values of the composites obtained can differ significantly. Larger π systems show stronger NLO effects but they are also geometrically larger. Therefore, incorporating a high concentration of molecules like substituted stilbens into the pore structure of molecular sieves turned out to be a difficult undertaking.

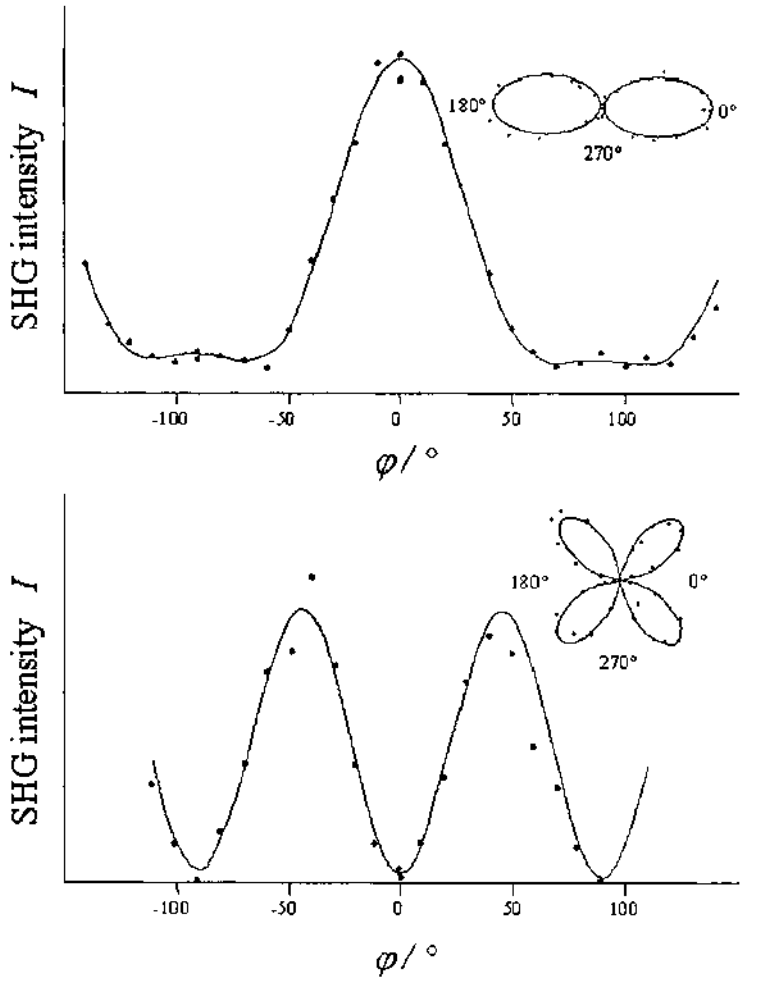

Fig. 9 Dependence of the SHG intensity on the polarization of the incident beam for the composite of DMABN and $AlPO_4$-5. The angle φ is measured between the polarization plane of the incident beam and the crystal axis. (Adapted from Ref. 126.)

E. Photochromic Switching

Photochromism is the reversible phototransformation of organic molecules between two forms with different absorption spectra (130). Photochromic materials are used in the areas of actinometry, security printing, light filtering, or optical data storage. For photochromic processes, a change in molecular orientation, molecular structure, or charge distribution due to different mechanisms is necessary. This change can be due to (a) cis-trans isomerization, (b) hydrogen tautomerism, (c) cyclization, (d) bond cleavage, (e) dissociation, (f) dimerization, (g) charge transfer, or (h) changes in the intermolecular arrangement (131).

A number of photochromic systems mainly based on cis-trans isomerization and bond cleavage reactions have been studied after incorporation into molecular sieves. They

have been prepared by adsorption of dyes, by crystallization inclusion, or by ship-in-the-bottle synthesis of photochromic molecules. The photochromic spiropyran 6-nitro-1′,3′,3′-trimethylspiro[2H-1]benzopyrane-2,2′-indoline was successfully synthesized in the faujasite supercages of NaY (132). Its photochromic properties are due to reversible bond cleavage of the closed colorless spiro form into the open, deeply colored merocyanine form. The conversion is triggered by UV light of different wavelengths and can be monitored by characteristic UV/vis spectra. In solution, the spiropyran molecule exists in the spiro form and is isomerized by irradiation with UV light to the colored merocyanine form. In the polar environment of molecular sieve pores, however, the molecule is stabilized in the zwitterionic merocyanine form and can be converted to the colorless spiropyran form by irradiation. A pronounced reversibility of the photochromic behavior was found. After irradiation of the colored dye-containing zeolite, the strong absorption at 550 nm is bleached, whereas a thermal relaxation in the dark recovered the characteristic absorption of the merocyanine form in the visible spectral range (58).

Photochromic properties as a result of cis-trans isomerization have been investigated after incorporation of olefins in faujasites and pentasil-type zeolites. A restricted rotational and translational motion of the olefin molecules stilbene and 1.4-diphenylbutadiene was found in the constrained environment of the zeolite pores (133). In ZSM-5 with smaller pores, the isomerization of *trans*-stilbene is more hindered than in NaY, as was shown by combined NMR and fluorescence lifetime studies (134–136). A photosensitized isomerization of *cis*-stilbene after intrazeolitic synthesis of the photoinduced electron-transfer sensitizer 2,4,6-triphenylpyrylium cation within the cages of zeolite Y has also been reported (137).

Photochromic azo group–containing composite materials have been extensively studied with respect to their optical properties. The efficient photoinduced processes are caused by trans-cis isomerization, which is reversible even in rigid matrices (130,138). As in various other media, two configurations of azobenzene (139) exist in pores of zeolites such as ZSM-5 (86,140), silicalite-1 (86), mordenite (141), zeolite X (142), Y (143,140), as well as in the molecular sieve $AlPO_4$-5 (86,144). The metastable *cis*-azobenzene is formed from the *trans*-azobenzene by a photoinduced isomerization process. After irradiation with UV light, leading to the cis isomer, the $\pi\pi^*$ band is diminished and blue shifted, whereas the intensity of the $n\pi^*$ band around 425 nm is increased (Fig. 10). Irradiation with blue light regenerates the thermodynamically stable trans isomer.

Pronounced photochromic effects have been found for azobenzene incorporated in the anisotropic channel structures of $AlPO_4$-5, ZSM-5, and silicalite-1 which provide a valuable basis for the further development of optical microswitches. However, photochromic changes of these composites are in most cases not sufficient for an application in optical switches for information processing because of destructive readout problems and thermal problems.

F. Photosensitive Refractive Index Switching

During the switching of photochromic materials, not only absorption spectra are altered as a result of different molecular or geometrical structures, but also dielectric properties or the refractive indices. Refractive index changes can effectively influence the flow of light through a medium. In devices, this can be realized electrically through the application of voltage, by mechanical changes, by photogeneration of charges, or by the use of heating effects. Organic polymers with thermosensitive refractive indices are currently being

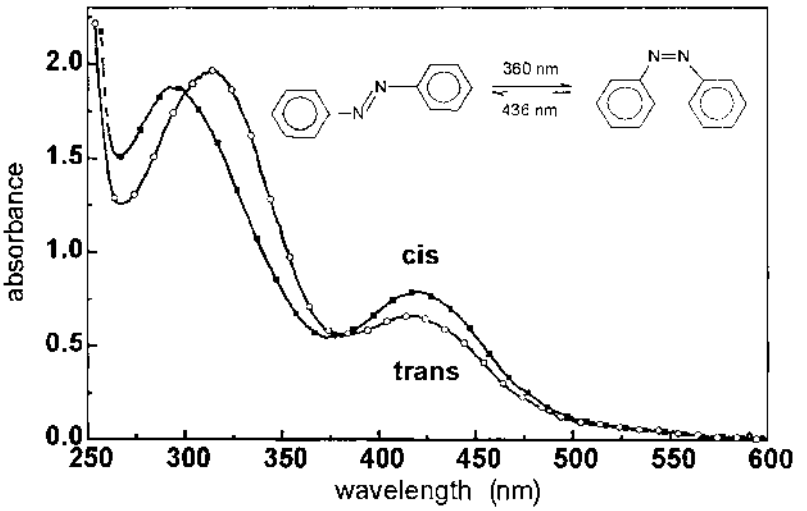

Fig. 10 Photochromism of azobenzene incorporated in ZSM-5. The microspectroscopic absorption of a dye-loaded zeolite microcrystal was measured after short-wavelength (cis isomer, solid squares) and long-wavelength (trans isomer, open circles) irradiation. (Adapted from Ref. 86.)

considered as switching components in optical fiber switching devices (145). These components could be replaced by photochromic materials that change their refractive index by optical stimulation only. They can be applied to various photonic devices, such as erasable optical memories or opto-optical switches and displays.

Incorporation of photosensitive guests into the pores of molecular sieves (43,134, 146,147) make zeolite-based composites interesting for photoswitchable materials. Refractive index changes resulting directly from the photochromic changes are, however, very small. This result is drastically changed if an ensemble of aligned guest molecules is switched within molecular sieve pores. In this case, an extremely high photosensitive change of the refractive index was found, caused by intrazeolitic photoinduced trans-cis isomerization of azobenzene (86). In addition to the photochromic behavior described in Sec. IV.E, different orientations of guest molecules occur after appropriate irradiation. These different orientations in the molecular sieve channels are caused by the different shape of the azobenzene isomers. The switching process leads to the changes in the optical transmission visible in Fig. 11, which is the quantification of different interference colors of the birefringent molecular sieve crystals observed between crossed polarizers. The dye-loaded $AlPO_4$-5 crystal investigated in the measurements shown in Fig. 11 appears green before irradiation, due to a maximal transmission at about 550 nm, but after short-wavelength irradiation it looks red, corresponding to a transmission at about 650 nm.

Interestingly, there is a wavelength (650 nm) for the composite crystal under study where the transmission changes from 2% to 95% after irradiation (see Fig. 11, top). Here the transmission of the setup can be switched between two stable states with a high contrast ratio using optical stimulation. This is an opto-optical switch realized on the micrometer scale.

The strong alteration of the birefringence upon irradiation was found to be a direct consequence of the alteration of the molecular alignment. The molecular sieve crystals in the trans state, which contains preferentially the better aligned rod-shaped *trans*-azoben-

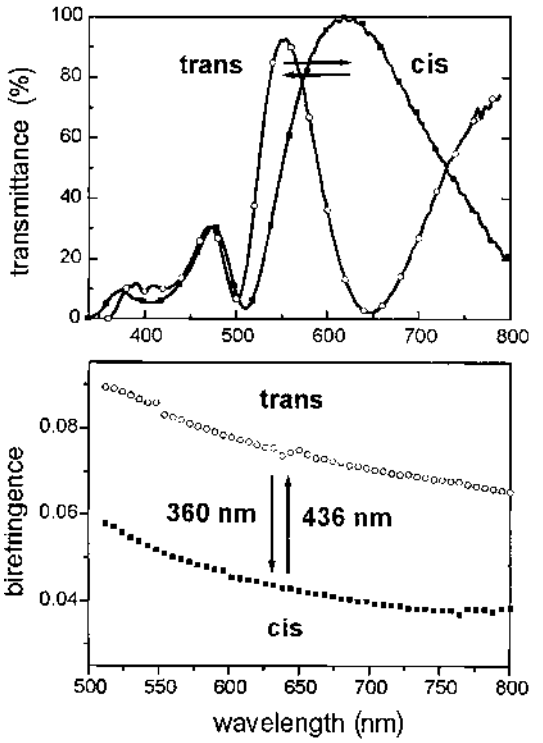

Fig. 11 Photosensitive birefringence of an azobenzene-loaded $AlPO_4$-5 microcrystal. Top: Transmission spectra of a crystal measured between two polarizers after irradiation with short- (solid squares) and long-wavelength (open circles) light. Bottom: Birefringence changes of the microcrystal determined from the transmission measurement using two parallel polarizers.

zene, show higher birefringence than the cis state composite encapsulating preferentially the bent *cis*-azobenzene molecules. These orientational rearrangements in molecular sieve channels increase the photosensitive refractive index changes compared with those resulting from the photochromic effect only. The type of the molecular sieve influences the magnitude and the characteristics of the switching process. This indicates an important role of the host–guest interactions in the isomerization process (151).

One of the main characteristics to be considered in developing photosensitive materials is the maximum refractive index change or the dynamic range of the effect. For $AlPO_4$-5 composites, photosensitive refractive index changes $\Delta n'$ up to 0.045 have been found from measurements of the birefringence between two polarizers of a microscope spectrometer as described in sec. III.C. The magnitude of the photosensitive effect in azobenzene-loaded $AlPO_4$-5 is remarkable and offers the possibility of realizing zeolite-based micro-optical switches. However, practical applications to the actual photonic devices require a critical evaluation of the organic/inorganic photosensitive materials from various points of views, including (a) stability of both switching states, (b) sensitivity, (c) response time, (d) reversibility of the effect, and (e) nondestructive readout capability (148). Some of these parameters have been investigated in order to check the properties of azobenzene-loaded $AlPO_4$-5 composites with photosensitive refractive index changes for their use as photoswitchable materials.

1. Switching-State Stability and Sensitivity

The stability of the switching states is of crucial interest for optical applications. Only the trans isomer of the photochromic azobenzene guest molecule is thermodynamically stable. After the photoinduced generation of the metastable cis isomer within the molecular sieve pores, azobenzene thermally relaxes to the stable trans isomer. This cis-to-trans relaxation can be monitored by UV/vis spectroscopy of the characteristic spectral changes as a function of time. Unfortunately, the disturbance of the thermal relaxation by the observation light during microspectroscopic investigations complicates the process (151). Taking this influence into consideration, the lifetimes $\tau_{1/2}$ of the metastable *cis*-azobenzene in different molecular sieve hosts were determined. It turns out that both the thermodynamically stable trans state as well as the metastable cis state can be considered as being long-term stable in the dark from the applicational point of view.

Another important parameter of photorefractive materials is sensitivity. The photorefractive sensitivity $S_{n'2}$ is defined as the magnitude of the refractive index change produced by a certain amount of irradiation energy (149). The sensitivity of the cis-to-trans as well as the trans-to-cis reaction of an azobenzene/$AlPO_4$-5 composite has been determined by observing the kinetics of the refractive index changes upon irradiation. The calculated values $S_{n'2} = -4.1$ and 6.5 cm^2/kJ, respectively, are comparable to those reported for inorganic photorefractive materials like lithium niobate (150).

2. Nondestructive Readout Capability and Reversibility

Destructive readout problems of an azobenzene/$AlPO_4$-5 microswitch are naturally minimized by the low spectral overlap between the switching light generating the two states of the microswitch and the readout light. One can choose the readout wavelength in the low-energy spectral range, e.g., at 750 nm. Nevertheless, minor destructive readout can also be detected in this system. In a repeated optical measurement of the cis state, an influence of the measurement light was indeed found (151). However, this effect strongly depends on the experimental conditions, which can be chosen in such a way that the readout of the cis state is possible several hundred times before it is destroyed. This capability of refractive index switches is a clear advantage over photochromic switches that always seem to suffer from destructive readout problems.

The reversibility of the zeolite-based photoswitchable material has been checked by alternating irradiation of a composite crystal with light of the wavelength 360 nm and 436 nm, generating the cis or the trans isomer of the azobenzene molecule, respectively. The difference of the birefringence in the cis and trans state composites changes only slightly with the number of cycles. The reversible photosensitive change in the refractive index of the composite material is preserved over several cycles as shown in Fig. 12 (151).

A quantification of the reversibility of photoswitchable compounds is the number of repetitions $N_{1/2}$ after which the switching effect has decreased to half the value of the first cycle. For the azobenzene/$AlPO_4$-5 composites, a value of about 300 was estimated from the measurements shown in Fig. 12. This value considerably exceeds $N_{1/2}$ of other photochromic organic/inorganic composites (152), but it requires further efforts to increase this quantity in order to design a useful material.

Regarding optical applications, azobenzene-loaded $AlPO_4$-5 nanocomposites fulfill important conditions for the construction of photoswitchable microdevices. Because of their large refractive index changes, their long-term stability, and reversibility of the switching states, they represent a first step in the development of all-optical microswitches based on dye-loaded zeolite single crystals.

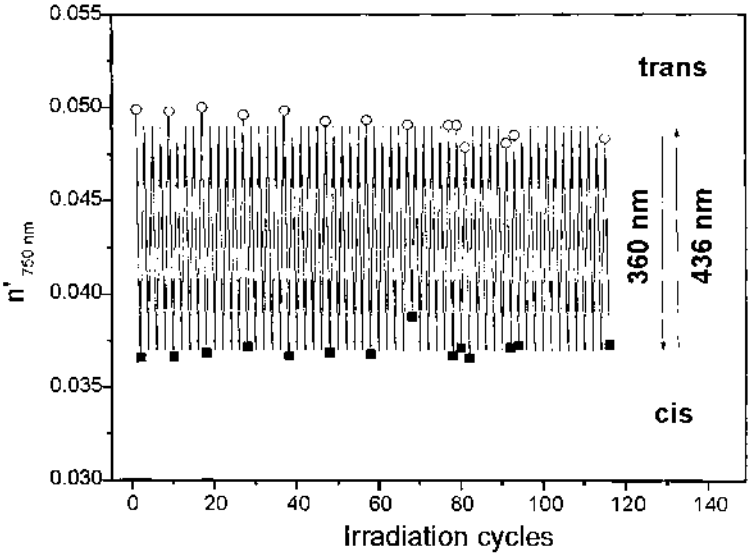

Fig. 12 The reversibility of the photosensitive switching process of an azobenzene/$AlPO_4$-5 crystal under alternating short-wavelength (360 nm; −■−) and long-wavelength irradiation (436 nm; −○−). (Adapted from Ref. 151.)

V. OUTLOOK

In recent years, a great deal of interest has been directed to the use of zeolites and related microporous solids in the development of ultraselective catalysts, clever design of chemical and biological sensors, and modified membranes. Zeolites can also act as effective host frameworks for encapsulating and organizing molecules, crystalline nanophases, and supramolecular entities inside the zeolite pores. The properties of zeolitic guest/host materials can be tuned through the selection of host structure, guest molecules, guest content, and distribution. Space confinement and host–guest interaction result in composite materials having novel optical, electronical, and magnetic properties of interest for the development of advanced materials.

Potential applications can, for example, be expected in the field of zeolite-based optical switches that route information in the form of light, rather than converting it to electronic signals as most of the current switches do. Optical switches are a critical bottleneck in the miniaturization of light-affecting devices that are indispensable for future communication systems. The described microporous host/organic guest systems demonstrate the potential of molecular sieve–based composites to be used in a new generation of high-efficiency optoelectronic and photonic devices such as light-harvesting systems, optochemical sensors, microlasers, frequency converters, as well as micro-optical switches based on zeolite single crystals.

ACKNOWLEDGMENT

The authors thank the German Science Foundation (DFG) for their support (RE 1203/2, Ma 1745/3, Ma 1745/4).

REFERENCES

1. GA Ozin. Adv Mater 6:71–76, 1994.
2. GD Stucky, JE MacDougall. Science 247: 669–678, 1990.
3. GA Ozin. Adv Mater 4:612–649, 1992.
4. G Schulz-Ekloff. Stud Surf Sci Catal 85:145–171, 1994.
5. G A Ozin, A Kuperman, A Stein. Angew Chem Int Ed Engl 28:359–376, 1989.
6. P Behrens, GD Stucky. In: JL Atwood, JED Davies, DD MacNicol, F Vögtle, JM Lehn, eds. Comprehensive Supramolecular Chemistry. Oxford: Pergamon Press, 1996, pp 722–768.
7. F Marlow, W Dong, K Hoffmann, J Loerke. In: F Schüth, KSW Sing, J Weitkamp, eds. Handbook of Porous Solids, Vol. 5, Weinheim: Wiley-VCH, 2002, pp 3029–3063.
8. U Simon, ME Franke. Micropor Mesopor Mater 41:1–36, 2000.
9. J Sauer, F Marlow, F Schüth. In: S Nalwa, ed. Handbook of Advanced Electronic and Photonic Materials and Devices, Vol. 6, New York: Academic Press, 2001, pp 153–172.
10. T Brar, P France, PG Smirniotis. Ind Eng Chem Res 40:1133–1139, 2001.
11. L Persaud, AJ Bard, A Campion, MA Fox, TE Mallouk, SW Webber, JM White. J Am Chem Soc 109:7309–7314, 1987.
12. J Schneider, D Fanter, M Bauer, C Schomburg, D Wöhrle, G Schulz-Ekloff. Micropor Mesopor Mater 39:257–263, 2000.
13. M Alvaro, H Garcia, S Corrent, JC Scaiano. J Phys Chem 102:7530–7534, 1998.
14. NB Castagnola, PK Dutta. J Phys Chem B 105:1537–1542, 2001.
15. S Engel, U Kynast, KK Unger, F Schüth. Stud Surf Sci Catal 84:477–483, 1994.
16. D Demuth, GD Stucky, KK Unger, F Schüth. Micropor Mater 3:473–487, 1995.
17. S Feng, R Xu. Acc Chem Res 34:239–247, 2001.
18. S Qiu, J Yu, G Zhu, O Terasaki, Y Nozue, W Pang, R Xu. Micropor Mesopor Mater 21:245–251, 1998.
19. RA Rakoczy, S Ernst, M Hartmann, Y Traa, J Weitkamp. Catal Today 49:261–266, 1999.
20. FS Xiao, S Qiu, W Pang, R Xu. Adv Mater 11:1091–1099, 1999.
21. G Finger, J Richter-Mendau, M Bülow, J Kornatowski. Zeolites 11:443–448, 1991.
22. S Radaev, W Joswig, WH Baur. J Mater Chem 6:1413–1418, 1996.
23. Ö Weiss, G Ihlein, F Schüth. Micropor Mesopor Mater 35–36:617–620, 2000.
24. JE Gilbert, A Mosset. Mater Res Bull 33:997–1003, 1998.
25. S Ferchiche, M Valcheva-Trykova, DEW Vaughan, J Warzywoda, A Sacco. J Cryst Growth 222:801–805, 2001.
26. C Shao, X Li, S Qiu, FS Xiao, O Terasaki. Micropor Mesopor Mater 39:117–123, 2000.
27. FF Gao, XT Li, GS Zhu, SL Qui, B Wei, CL Shao, O Terasaki. Mater Lett 48:1–7, 2001.
28. CL Shao, XT Li, SL Qiu, FS Xiao. Micropor Mesopor Mater 33:215–222, 1999.
29. I Girnus, K Jancke, R Vetter, J Richter-Mendau, J Caro. Zeolites 13:33–39, 1995.
30. I Girnus, MM Pohl, J Richter-Mendau, M Schneider, M Noack, D Venske, J Caro. Adv Mater 7:711–714, 1995.
31. J Warzywoda, N Bac, JC Jansen, A Sacco. J Cryst Growth 220:140–149, 2000.
32. J Warzywoda, M Valcheva-Traykova. GA Rosetti Jr, N Bac, R Joesten, SL Suib, A Sacco Jr. J Cryst Growth 220:150–160, 2000.
33. J Warzywoda, N Bac, GA Rosetti Jr., N van der Puil, JC Jansen, H van Bekkum, A Sacco Jr. Micropor Mesopor Mater 38:423–432, 2000.
34. EN Coker, JC Jansen, F DiRenzo, F Fajula, JA Martens, PA Jacobs, A Sacco Jr. Micropor Mesopor Mater 46:223–236, 2001.
35. D Wöhrle, AK Sobbi, O Franke, G Schulz-Ekloff. Zeolites 15:540–550, 1995.
36. G Ihlein, F Schüth, O Krauß, U Vietze, F Laeri. Adv. Mater 10:1117–111,1998.
37. R Hoppe, G Schulz-Ekloff, D Wöhrle, C Kirschhock, H Fuess, L Uytterhoeven, R Schoonheydt. Adv Mater 7:61–64, 1995.
38. S Wohlrab, R Hoppe, G Schulz-Ekloff, D Wöhrle. Zeolites 12:862–865, 1992.
39. S Kowalak, KJ Balkus. Coll Czech Chem Commun 57:774–780, 1992.

40. M Ehrl, FW Deeg, C Bräuchle, O Franke, A Sobbi, G Schulz-Ekloff, D Wöhrle. J Phys Chem 98:47–52, 1994.
41. D Wöhrle, G Schulz-Ekloff. Adv Mater 6:875–880, 1994.
42. M Bockstette, D Wöhrle, I Braun, G Schulz-Ekloff. Micropor Mesopor Mater 23:83–96, 1998.
43. R Hoppe, G Schulz-Ekloff, D Wöhrle, C Kirschhock, H Fuess. Langmuir 10:1517–1523, 1994.
44. I Braun, G Schulz-Ekloff, M Bockstette, D Wöhrle. Zeolites 19:128–132, 1997.
45. I Braun, G Ihlein, F Laeri, JU Nöckel, G Schulz-Ekloff, F Schüth, U Vietze, Ö Weiss, D Wöhrle. Appl Phys B 70:335–343, 2000.
46. S Thiele, S Radaev, K Hoffmann, R Vetter, F Marlow. Zeolites 19:190–196, 1997.
47. V Ramamurthy, DR Sanderson, DF Eaton. J Am Chem Soc 115:10438–10441, 1993.
48. GH Kühl. In: J Weitkamp, L Puppe, eds. Catalysis and Zeolites. Berlin: Springer-Verlag, 1999, pp 81–179.
49. R Hoppe, G Schulz-Ekloff, D Wöhrle, ES Shpiro, OP Tkachenko. Zeolites 13:222–228, 1993.
50. D Brühwiler, N Gfeller, G Calzaferri. J Phys Chem B 102:2923–2929, 1998.
51. G Calzaferri, N Gfeller. J Phys Chem 96:3428–3435,1992.
52. N Gfeller, S Megelski, G Calzaferri. J Phys Chem B 103:1250–1257, 1999.
53. A Kunzmann, R Seifert, G Calzaferri. J Phys Chem B 103:18–26, 1999.
54. K Ho, HS Lee, BC Leano, T Sun, K Seff. Zeolites 15:377–381, 1995.
55. ML Cano, A Corma, V Fornes, H Garcia, M Mirinda, C Baerlocher, C Lengauer. J Am Chem Soc 118:11006–11013, 1996.
56. JL Meinershagen, T Bein. J Am Chem Soc 121:448–449, 1999.
57. C Schomburg, D Wöhrle, G Schulz-Ekloff. Zeolites 17:232–236, 1996.
58. I Casades, S Constantine, D Cardin, H Garcia, A Gilbert, F Marquez. Tetrahedron 56:6951–6956, 2000.
59. SD Cox, GD Stucky. J Phys Chem 95:710–720, 1991.
60. HL Frisch, JE Mark. Chem Mater 8:1735–1738, 1996.
61. CG Wu, T Bein. Science 264:1757–1759, 1994.
62. P Enzel, T Bein. J Phys Chem 93:6270–6272, 1989.
63. T Bein, P Enzel. Angew Chem 101:1737–1738, 1989.
64. A Gräser, S Spange. Chem Mater 10:1814–1819, 1998.
65. KT Jackson, RF Howe. Zeolites Micropor Cryst 83:187–194, 1994.
66. V Ramamurthy. In: V Ramamurthy, ed. Photochemistry in Organized and Constrained Media. New York: VCH, 1991, pp 429–493.
67. SD Cox, TE Gier, GD Stucky, J Bierlein. J Am Chem Soc 110:2986–2987, 1988.
68. K Hoffmann, F Marlow, J Caro, S Dähne. Zeolites 16:138–141, 1996.
69. K Hoffmann, F Marlow, J Caro. Zeolites 16:281–286, 1996.
70. C Striebel, K Hoffmann, F Marlow. Micropor Mater 9:43–50, 1997.
71. K Hoffmann, D Prescher, F Marlow. J Inf Rec 24:191–196, 1998.
72. S Megelski, A Lieb, M Pauchard, A Drechsler, S Glaus, C Debus, AJ Meixner, G Calzaferri. J Phys Chem B 105:25–35, 2001.
73. K Hoffmann, F Marlow, J Caro. J Fluoresc 4:75–77, 1994.
74. C Domingo, J Garcia-Carmona, J Llibre, R Rodriguez-Clemente. Adv Mater 10:672–676, 1998.
75. F Marlow; J Caro. Zeolites 12:433–434, 1992.
76. G van de Goor, K Hoffmann, S Kallus, F Marlow, F Schüth, P Behrens. Adv Mater 8:65–69, 1996.
77. GG Lindner, K Hoffmann, K Witke, D Reinen, C Heinemann, W Koch. J Solid State Chem 126:50–54, 1996.
78. I Girnus, K Hoffmann, F Marlow, J Caro, G Döring. Micopor Mater 2:537–541, 1994.
79. I Girnus, K Hoffmann, F Marlow, J Caro. GIT Special 96:49–51, 1996.
80. J Caro, F Marlow, M Wübbenhorst. Adv Mater 6:413–416, 1994.

81. CO Arean. Comm Inorg Chem 22:241–273, 2000.
82. F Marlow, K Hoffmann, GG Lindner, I Girnus, G van de Goor, J Kornatowski, J Caro. Micropor Mater 6:43–49 1996.
83. Y Ikemoto, Y Nozue, S Qui, O Tersaki, T Kodaira, Y Kiyozumi, T Yamamoto. Mater Sci Eng A217/218:151–154, 1996.
84. VV Poborchii, MS Ivanova, SS Ruvimov. Stud Surf Sci Catal 84:2285–2293, 1994.
85. C Janiak, TG Scharman, P Albrecht, F Marlow, R Macdonald. J Am Chem Soc 118:6307–6308, 1996.
86. K Hoffmann, F Marlow, J Caro. Adv Mater 9:567–570, 1997.
87. F Schüth. J Phys Chem 96:7493–7496, 1992.
88. WPJH Jacobs, DG Demuth, SA Schunk, F Schüth. Micropor Mater 10:95–109, 1997.
89. F Marlow, D Demuth, G Stucky, F Schüth. J Phys Chem 99:1306–1310, 1995.
90. G Müller, J Bodis, G Eder-Mirth, J Kornatowski, JA Lercher. J Mol Struct 410–411:173–178, 1997.
91. YS Lin, N Yamamoto, Y Choi, T Yamaguchi, T Okubo, SI Nakao. Micopor Mesopor Mater 38:207–220, 2000.
92. F Marlow, W Hill, J Caro. J Raman Spectrosc 24:603–608, 1993.
93. VV Poborchii. J Phys Chem Solids 55:737–743, 1994.
94. ZK Tang, MMT Loy, T Goto, J Chen, R Xu. Solid State Commun 101:333–336, 1997.
95. V Poborchii, A Kobolov, H Oyanagi, S Romanov, K Tanaka. Nanostruct Mater 10:427–436, 1998.
96. VV Poborchii, AV Kobolov, J Caro, VV Zhuravlev, K Tanaka. Chem Phys Lett 280:17–23, 1997.
97. CC Eggeling, J Widengren, R Rigler, CAM Seidel. In: W Rettig, B Strehmel, S Schrader, H Seifert, eds. Applied Fluorescence in Chemistry, Biology and Medicine, Berlin: Springer-Verlag, 1999, pp 195–240.
98. A Dubois, M Canva, A Brun, F Chaput, JP Boilot. Synth Met 81:305–308, 1996.
99. A Vaidyalingam, PK Dutta. Anal Chem 72:5219–5224, 2000.
100. M Pauchard, A Devaux, G Calzaferri. Chem Eur J 6:3456–3470, 2000.
101. L Cot, A Ayral, J Durand, C Guizard, N Hovnanian, A Julbe, A Larbot. Solid State Sci 2:313–334, 2000.
102. YSS Wan, JLH Chau, A Gavriilidis, KL Yeung. Micropor Mesopor Mater 42:157–175, 2001.
103. S Mintova, SY Mo, T Bein. Chem Mater 13:901–905, 2001.
104. MB Berry, BE Libby, K Rose, KH Haas, RW Thompson. Micropor Mesopor Mater 39:205–217, 2000.
105. G Binder, L Scandella, J Kritzenberger, J Gobrecht. J Phys Chem B 101:483–490, 1997.
106. JC Scaiano, H Garcia. Acc Chem Res 32:783–793, 1999.
107. JL Meinershagen, T Bein. J Am Chem Soc 121:448–449, 1999.
108. B Meier, T Werner, I Klimant, OS Wolfbeis. Sensors Actuators B 29:240–245, 1995.
109. JT Remillard, JR Jones, BD Poindexter, CK Narula, WH Weber. Appl Opt 38:5306–5309, 1999.
110. R Berger, C Gerber, HP Lang, JK Gimzewski. Microelectronic Eng 35:373–379, 1997.
111. H Baltes, CA Leme. In: W Göpel, J Hesse, JN Zemel eds. Micro- and Nanosensor Technology/Trends in Sensor Markets, Vol. 8, Weinheim: VCH, 1995, p 52.
112. L Scandella, G Binder, T Mezzacasa, J Gobrecht, R Berger, HP Lang, C Gerber, JK Gimzewski, JH Koegler, JC Jansen. Micropor Mesopor Mater 21:403–409, 1998.
113. V Balzani, F Scandola. Supramolecular Photochemistry. New York: Horwood, 1990, pp 355–385.
114. G Calzaferri. Chimia 52:525–532, 1998.
115. PK Dutta, M Ledney. Progr Inorg Chem 44:209–271, 1997.
116. JR Kincaid. Chem Eur J 6:4055–4061, 2000.
117. JS Krueger, JE Mayer, TE Mallouk. J Am Chem Soc 110: 8232–8234, 1988.
118. NB Castagnola, PK Dutta. J Phys Chem B 102:1696–1702, 1998.

119. M Vitale, NB Castagnola, NJ Ortins, JA Brooke, A Vaidyalingam, PK Dutta. J Phys Chem B 103: 2408–2416, 1999.
120. F Binder, G Calzaferri, N Gfeller. Solar Energy Mater Solar Cells 38:175–186, 1995.
121. G Calzaferri, D Brühwiler, S Megelski, M Pfenninger, M Pauchard, B Hennessy, H Maas, A Devaux, U Graf. Solid State Sci 2:421–447, 2000.
122. U Vietze, O Krauß, F Laeri, G Ihlein, F Schüth, B Limburg, M Abraham. Phys Rev Lett 81:4628–4631, 1998.
123. G Ihlein, F Schüth, O Krauss, U Vietze, F Laeri. Adv Mater 10:1117–1119, 1998.
124. F Laeri, JU Nöckel. In: S Nalwa, ed. Handbook of Advanced Electronic and Photonic Materials and Devices, Vol. 6. New York: Academic Press, 2001.
125. L Werner, J Caro, G Finger, J Kornatowski. Zeolites 12:658–663, 1992.
126. F Marlow, J Caro, L Werner, J Kornatowski, S Dähne. J Phys Chem 97:11286–11290, 1993.
127. G Reck, F Marlow, J Kornatowski, W Hill, J Caro. J Phys Chem 100:1698–1704, 1996.
128. F Marlow, M Wübbenhorst, J Caro. J Phys Chem 98:12315–12319, 1994.
129. GF Klap, SM van Klooster, M Wübbenhorst, JC Jansen, H van Bekkum, J van Turnhout, J Phys Chem B 102: 9518–9521, 1998.
130. JA Delaire, K Nakatani. Chem Rev 100:1817–1845, 2000.
131. GJ Ashwell. In: RJH Clark, RE Hester, eds. Spectroscopy of New Materials, Chichester: Wiley, 1993, pp 61–85.
132. D Wöhrle, G Schulz-Ekloff, I Braun, C Schomburg, F Laeri, U Vietze, M Ganschow, Y Rohlfing, T Bogdahn-Rai. J Inform Rec 25:87–94, 2000.
133. V Ramamurthy. Chimia 46:359–376, 1992.
134. V Ramamurthy, JV Caspar, DR Corbin, DF Eaton, JS Kauffman, JS Dybowski. J Photochem Photobiol A 51:259–265, 1990.
135. M Baldovi, A Corma, H Garcia, V Marti. Tetrahedron Lett 35:9447–9450, 1994.
136. EH Ellison, JK Thomas. J Phys Chem B 105:2757–2760, 2001.
137. A Corma, V Fornes, H Garcia, MA Miranda, J Primo, M Sabater. J Am Chem Soc 116:2276–2280, 1994.
138. F Chaput, J Biteau, K Lahlil, JP Boilot, B Darracq, Y Levy, J Peretti, VI Safarov, G Parent, A Fernandez-Acebes, JM Lehn. Mol Cryst Liq Cryst 344:77–83, 2000.
139. H Rau. In: JF Rabek, ed. Photochemistry and Photophysics, Vol. 4. Boca Raton, FL: CRC Press, 1990, pp 120–141.
140. A Corma, H Garcia, S Iborra, V Marti, MA Miranda, J Primo. J Am Chem Soc 115:2177–2180, 1993.
141. M Kojima, T Takagi, T Goshima. Mol Cryst Liq Cryst 344:179–184, 2000.
142. K Weh, M Noack, K Hoffmann, KP Schröder, J Caro. Micropor Mesopor Mater 54:15–26, 2002.
143. Y Kuriyama, S Oishi. Chem Lett 1999:1045–1046, 1999.
144. Z Lei, A Vaidyalingam, PK Dutta. J Phys Chem B 102:8557–8562, 1998.
145. T Watanabe, N Ooba, S Hayashida, T Kurihara, S Imamura. J Lightwave Tech 16:1049–1055, 1998.
146. K Maruyama, T Tsuzuki, M Yao, H Endo. Surf Rev Lett 3:711–715, 1996.
147. A Lalitha, K Pichumani, C Srinivasan. J Photochem Photobiol A 134:193–197, 2000.
148. N Tamai, H Miyasaka. Chem Rev 100:1875–1890, 2000.
149. P Günther, JP Huignard. Photorefractive Materials and Their Applications, Vols. 1 & 2. Berlin: Springer-Verlag, 1988 and 1989, pp 1–53.
150. F Marlow, K Hoffmann. Ber Bunsenges Phys Chem 101:1731–1734, 1997.
151. K Hoffmann, U Resch-Genger, F Marlow. Micropor Mesopor Mater 41:99–106, 2000.
152. H Tagaya, T Nagaoka, T Kuwahara, M Karasu, J Kadokawa, K Chiba. Micropor Mesopor Mater 21:395–402, 1998.